Time Domain Unsteady Incompressible Cascade Airfoil Theory for Helicopter Rotors in Hover

M. A. H. Dinyavari* and P. P. Friedmann†
University of California, Los Angeles, Los Angeles, California

A detailed derivation of a finite-time arbitrary-motion incompressible casade theory is presented for both Laplace and frequency domains. Such theories are useful for both aeroelastic stability and response calculations. The generalized cascade lift deficiency function C'' is shown to be consistent with the generalized Theodorsen's lift deficiency function when the wake spacing approaches infinity or when the reduced frequency tends to infinity; it also yields a correct value for the zero reduced frequency limit. Efficient numerical procedures are presented for the evaluation of the cascade lift deficiency function. Numerical examples comparing the cascade lift deficiency function with Loewy's rotary-wing lift deficiency function in frequency domain are presented. Pade approximants of the cascade lift deficiency function are constructed using a Bode plot approach that allows for complex poles. A general purpose optimization program is used to determine the coefficients of the approximant.

Nomenclature

a = lower limit of integration for frequency domain cascade theory

$\bar{a}bR$ = cross-sectional elastic center (E.C.) offset from midchord

a_m = coefficients in the numerator of the rational approximation for the lift deficiency function

b_m = coefficients in the denominator of the rational approximation for the lift deficiency function

bR = blade semichord length

$C''(\bar{s},\bar{T}_{Re},\bar{T}_{He})$, $C''(ik,\bar{T}_{Re},\bar{T}_{He})$ = casade lift deficiency function in the Laplace and frequency domains

$D(ik)$ = denominator polynomial of rational approximation for the lift deficiency function

F'',G'' = real and imaginary parts of cascade lift deficiency function

$F(\bar{s}:n,m,\bar{T}_R,\bar{T}_H)$ = family of double integrals

$F''_{\text{app}},G''_{\text{app}}$ = real and imaginary parts of rational approximant to the lift deficiency function

$f_m(\bar{\phi})$ = basis functions of the Glauert series

H^*,H_e^* = vertical wake spacing beneath the rotor in cascade wake model for single and multibladed rotors: $h_e = h/Q$; $h = [2\pi U_{PO}/\Omega]$; $(\bar{\ }) = (\ )/bR$

$h,h_e,\bar{h},\bar{h}_e$ = vertical wake spacing beneath the rotor in Loewy's model for single and multibladed rotor: $h_e = h/Q$; $h = [2\pi U_{po}/\Omega]$; $(\bar{\ }) = (\ )/bR$

$\Delta h(t)$ = vertical displacement of elastic center of the airfoil, positive downward

I = $\sqrt{-1}$

$I(t:n,m),I(\xi^*:n,m)$ = influence function of a vortex lying on the nth vortex sheet at ξ^* on the mth Fourier component of the wake-induced downwash velocity λ_m

$ID(ik:n,m,\bar{T}_{Re},\bar{T}_{He})$ = family of double integrals associated with the denominator of the cascade-wake lift deficiency function

$IMD(k)$ = imaginary part of the denominator polynomial in a rational approximation to the lift deficiency function

$IMN(k)$ = imaginary part of the numerator polynomial in a rational approximation to the lift deficiency function

$IN(ik:n,m,\bar{T}_{Re},\bar{T}_{He})$ = family of double integrals in the numerator of the cascade-wake lift deficiency function

$K_n(\ )$ = modified Bessel function of the second kind of nth order

k = reduced frequency: $k = \omega bR/U_{TO}$

L,L_C,L_{NC} = total, circulatory and noncirculatory components of the lift: $L = L_C + L_{NC}$

L_Q,L_W = quasisteady and wake components of the circulatory lift: $L_C = L_Q + L_W$

$\mathscr{L}$ = Laplace transform

$N(ik)$ = numerator polynomial of the rational approximation for the lift deficiency function

NL = number of wake layers beneath the rotor included in the cascade-wake lift deficiency function

NP = number of poles in the Pade approximant of the lift deficiency function

P = pressure

P_u,P_ℓ = pressure on the upper and lower surfaces of the airfoil, respectively

Q = number of blades

$Q(t),Q(s)$ = downwash velocity at the 3/4-chord point: $Q(s) = \mathscr{L}[Q(t)]$

R = blade radius

Received Nov. 25, 1986; revision received Dec. 2, 1987.

*Visiting Lecturer, Mechanical, Aerospace, and Nuclear Engineering Department, and Principal Engineer/Scientist, McDonnell Douglas Aircraft Co., Long Beach, CA. Member AIAA.

†Professor and Chairman, Mechanical, Aerospace, and Nuclear Engineering Department. Associate Fellow AIAA.

$RD(k)$, $RN(k)$ = real part of denominator and numerator polynomials, respectively, in a rational approximation of the lift deficiency function

$r, r_e, \bar{r}, \bar{r}_e$ = radial station of blade section: $r_e = (r/Q)$; $(\bar{}) = ()/bR$

$s, \bar{s}$ = Laplace transform variable: $\bar{s} = (sbR/U_{TO})$

T_H, T_{HE} = time required for a fluid particle to travel one wake spacing with the mean oncoming flow velocity: $T_H = H^*/U_{TO}$; $T_{He} = H_e^*/U_{TO}$

$\bar{T}_H, \bar{T}_{He}, \bar{T}_R, \bar{T}_{Re}$ = nondimensionalized T_H, T_{He}, T_R, T_{Re} with respect to T_{sc}: $(\bar{}) = ()/(T_{sc})$

T_R, T_{Re} = time required for fluid particle to travel the distance between identical airfoils on consecutive blades with the mean oncoming flow velocity: $T_R = 2\pi r/U_{TO}$; $T_{Re} = 2\pi r_e/U_{TO}$

T_{sc} = time required for fluid particle to travel the semichord length bR with the mean oncoming flow velocity: $T_{sc} = bR/U_{TO}$

t, t', τ = time

$U_T(t), U_P(t)$ = freestream velocity in x^*, and negative z^*directions, respectively: $U_T(t) = U_{TO} + \Delta U_T(t)$; $U_p(t) = U_{PO} + \Delta U_p(t)$

U_{TO} = constant portion of freestream velocity

$W_a(x^*,\tau), W_a(\bar{\phi},\tau)$ = upwash velocity distribution over the airfoil

$W_{am}(\tau)$ = Fourier coefficients of W_a

$W_b(x^*,\tau), W_b(\bar{\phi},\tau)$ = downwash velocity distribution on the airfoil induced by the bound vortex system

$X_A, \bar{X}_A$ = offset between the elastic center and the aerodynamic center in blade cross section: $\bar{X}_A = X_A/bR$

$X_n^*(\tau)$ = location of trailing edge of the wake behind the nth imaginary airfoil below the reference airfoil at time $t = \tau$ for cascade wake

$X_0^*(\tau)$ = location of trailing edge of the wake behind the reference airfoil at time $t = \tau$

x^*, z^* = coordinate axes in plane of the airfoil

$\alpha(t), \alpha_0, \Delta\alpha(t)$ = angle of incidence of the airfoil at the elastic center, measured clockwise from the horizontal x^* axis: $\alpha(t) = \alpha_0 + \Delta\alpha(t)$ where α_0 is the constant part, and $\Delta\alpha$ is time varying

$\Gamma(\tau), \Gamma(t)$, $\Gamma_{NC}^{(1)}(\tau), \Gamma_{NC}^{(2)}(\tau)$, $\Gamma_C^{(1)}(\tau), \Gamma_C^{(2)}(\tau)$ = various integrals of bound vortex over the airfoil in cascade-wake theory

$\Gamma, \Gamma_Q, \Gamma_W$ = total, quasisteady, and wake-induced circulation about the airfoil, respectively

∂ = partial derivative

$\lambda(\xi^*,\tau)$ = induced downwash velocity due to shed wakes behind and below the airfoil

$\lambda_m(\tau), \dot{\lambda}_m(\tau)$ = Fourier coefficients of the shed wake-induced downwash velocity over the airfoil and its time derivative

$\xi^*(\tau, t', n)$ = location of the vortex shed behind the nth imaginary airfoil at time $t = t'$ observed at time $t = \tau$

ρ_A = air density

$\Upsilon_a(\xi^*,\tau), \Upsilon_b(\xi^*,\tau)$ = bound vortex strength, positive clockwise

$\Upsilon_{bc}, \Upsilon_{bnc}$ = circulatory and noncirculatory portions of bound vortex strength shed at time $t = t'$

$\Upsilon_t(t')$ = trailing edge vortex strength shed at time $t = t'$

$\Upsilon_{WN}(\xi^*,\tau)$ = shed wake vortex strength behind the nth imaginary airfoil at time $t = \tau$, positive clockwise

ψ = azimuth angle of blade measured from straight aft position, also nondimensional time: $\psi = \Omega t$

Ω = rotor speed of rotation

$(\dot{})$ = differentiation with respect to time t

Introduction

PROPER modeling of unsteady aerodynamic effects is an important ingredient in aeroelastic stability and response calculation for rotary wing applications. Until recently, all unsteady aerodynamic theories used in rotary-wing applications were based on the assumption of simple harmonic motion. An important shortcoming of these theories is that they are suitable only for determining aeroelastic stability boundaries, since the assumption of simple harmonic motion holds only at the stability boundaries. Thus, these theories are not capable of predicting damping levels at subcritical condition. Furthermore, the modeling of aeroservoelastic systems, where an active control system is modeled in conjunction with the aeroelastic system, requires finite-state time-domain unsteady aerodynamics.

In this paper the term "finite-state time-domain aerodynamics" refers to theories that express unsteady airloads in the time domain in terms of a finite number of augmented state variables, in addition to the airfoil (or blade) physical degrees of freedom. The role of these augmented state variables is to convey information on the effects of the unsteady wake. The term "arbitrary finite-time motion" is used here to refer to a motion that has commenced at some previous finite time and has an arbitrary form. The arbitrary form of motion includes both growing and decaying oscillations with a certain frequency, as well as any other general transient response.

Three incompressible finite-time arbitrary-motion airfoil theories, suitable for coupled flag-lag-torsional aeroelastic analysis of rotary wings in hover and forward flight, were briefly outlined in Ref. 1. These were: 1) a generalized version of Greenberg's theory,[2,3] 2) a generalized version of Loewy's theory[4] and its finite-state time-domain approximation, and 3) a generalized cascade theory for hover.

For relatively lightly loaded rotors in hover, the wakes shed from other blades in the same revolution and wakes shed in previous revolutions tend to remain in the vicinity of the rotor disk, and the effect of the returning wake has to be taken into account. The first theory to model the influence of the layers of the shed vorticity beneath the rotor for the case of hover was developed by Lowey.[4] This theory represents a generalization of Theodorsen's theory to rotary wing applications, and thus is based on the assumption of simple harmonic blade motion. The intertwined helical wakes shed by previous blades or the reference blade in previous revolutions was idealized by a series of vortex sheets, infinite in number, parallel to the rotor disk, which extend to infinity on both sides of the airfoil representing a blade cross section. Recently this theory was extended to the arbitrary motions in Refs. 1 and 5. However, it has been pointed out[1,5] that the wake model postulated in Loewy's theory, which extends to infinity on both sides, is not compatible with the finite-time arbitrary-motion representation of the blade dynamics. The time delays between the wake layers can be represented by a relative horizontal shift between the wake layers in the two-dimensional idealization of the helical wake.

Although the extension of the wake aft of the trailing edge is natural, due to steady-state motion, the extension of the wake layers forward was a mathematical artifice introduced by Loewy to allow closed form analytical solutions for various wake integrals. The extension of the wake forward would be invalid, especially in the indicial lift calculations and short-time transient response analysis. Furthermore, in calculating a rotary-wing indicial lift function directly from Loewy's lift deficiency function, following Garrick's derivation of Wagner function,[1] various integrals of C' have to be evaluated from $-\infty < k < \infty$. Some of the improper integrals used in derivation of the Loewy's theory[4] diverge and become indeterminate[1] for $k < 0$. The zero-frequency limit of the Loewy's lift deficiency function is important for its generalization to the time domain. Some problems with this limit have been noted in Refs. 1 and 5. Thus, Loewy's wake model is not consistent with arbitrary motion type aerodynamics. The cascade-wake model used in this study is more appropriate for the derivation of finite-time arbitrary-motion aerodynamics of helicopter rotor blades in hover. In Refs. 1 and 5, three different techniques were used to construct the Pade approximants for Loewy's lift deficiency function: 1) Dowell's quadratic least squares technique,[6] 2) Vepa's quadratic least squares technique,[7] and 3) general nonlinear least squares approach using the Fletcher-Reeves unconstrained optimization algorithm. These techniques failed to capture the oscillatory behavior of the real and imaginary parts of Loewy's lift deficiency function. This can be attributed to three reasons: first, methods 1) and 2) above were developed for fixed-wing applications; second, method 1) can only handle real poles; third, the optimization algorithm used in method 3) was not suitable for solving problems with many local minima.

Recently, Venkatesan and Friedmann[8,9] have shown that the oscillatory nature of the rotary-wing lift deficiency function is associated with the presence of complex poles. Using a Bode plot technique to identify the number of complex poles and their approximate locations,[8,9] high quality approximations to Loewy's lift deficiency function capable of capturing its oscillatory behavior were obtained.

This paper has two objectives: 1) to present a complete derivation of the finite-time arbitrary-motion cascade theory and compare it to Loewy's theory, and 2) to develop an accurate finite-state time-domain representation of the loads, using the improved Pade approximant technique developed in Refs. 8 and 9.

Accurate closed form binomial approximations are used to develop an efficient combined analytical and numerical technique for the evaluation of the lift deficiency function in the frequency domain. A detailed comparison of the cascade theory with Loewy's theory is presented. Pade approximants of cascade lift deficiency function are constructed using the Bode plot approach described in Refs. 8 and 9, which allows for complex poles. A general purpose optimization program containing a wide variety of algorithms is employed to minimize the error function for the determination of the coefficient of approximant. This allows for considerable flexibility in selecting the optimization scheme appropriate for the rotary-wing class of problems.

Concise Derivation of the Cascade Theory

Wake Structure, Assumptions, and Approach

The finite-time cascade model consists of a wake in which a finite number of identical, staggered, imaginary airfoils are assumed to be flying beneath the rotor. A schematic representation of the wake model for a multibladed rotor, where all blades perform the same motion (collective mode), is shown in Fig. 1. The cascade wake model for finite-time arbitrary motion used in this derivation is similar to the wake structure assumed by Hammond.[10] However, it should be noted that the Hammond model is appropriate for the frequency domain, whereas the model used here is appropriate for the time domain. Reference 10 uses an acceleration potential approach to obtain the compressible unsteady aerodynamic loads, acting on two-dimensional rotor blade cross sections undergoing simple harmonic motions in hover. In the finite-time cascade-wake model, where a velocity potential approach is used, each airfoil is leading the previous one by the distance $(2\pi r)/Q$. The wakes behind the reference airfoil and each of the imaginary airfoils are of finite length, corresponding to the time elapsed since the motion has commenced.

Using this wake model, the integral equation of downwash for an airfoil undergoing coupled flap-lag-torsional motion about a nonzero pitch angle in a stream having time-varying oncoming and inflow velocities is formulated. The position of shed vortices behind the airfoil in each parallel wake layer is assumed to be determined by the mean velocity, whereas their instantaneous velocity is given by the time-varying oncoming velocity. Thus, the fore and aft excursions of the wake are partially taken into account. This is similar to the wake assumption used in the derivation of generalized Greenberg theory, described in Refs. 1 and 5.

The integral equation of the downwash is formulated using an approach that is similar to Johnson's derivation of Theodorsen's theory (Sec. 10 of Ref. 11). The integral equation of downwash is solved using the Söhngen inversion integral and a Fourier series method.

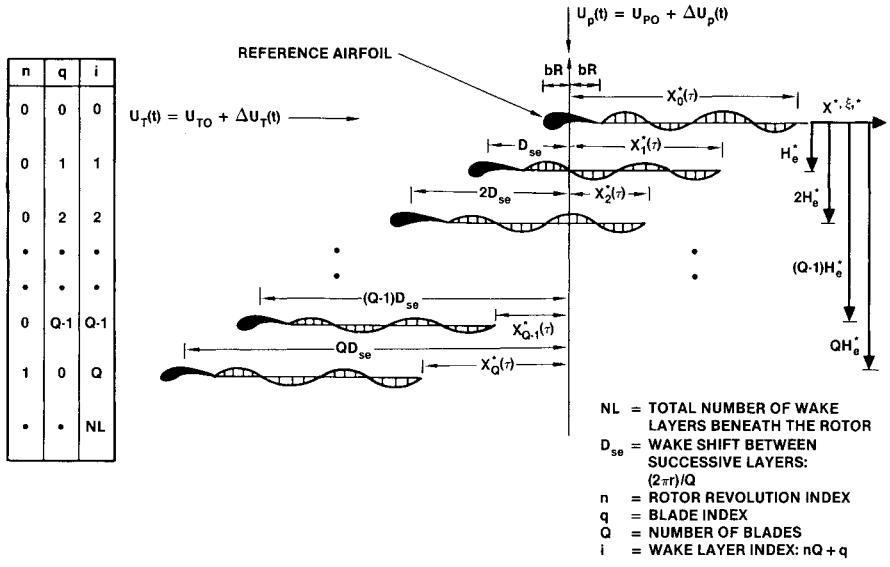

Fig. 1 Schematic representation of cascade-wake model for multibladed rotor undergoing arbitrary motion.

Formulation of the Theory

The geometry of motion of a typical airfoil is shown in Fig. 2. The governing equations consist of: 1) the boundary condition of zero disturbance upstream at infinity, 2) tangent flow velocity over the reference airfoil, 3) Kutta condition at the trailing edge of the reference airfoil, 4) zero pressure discontinuity on the wake, and 5) Kelvin's theorem of conversation of circulation. For mathematical convenience, the case of single-bladed rotor, $Q = 1$, is considered first.

The condition of tangent flow to the airfoil surface leads to an expression for the upwash velocity on the surface of the airfoil in the form of a Fourier series given by[5]

$$W_a(\bar{\phi},t) = \sum_{m=0}^{\infty} W_{am}(t)\cos(m\bar{\phi}) \tag{1}$$

where

$$W_{am}(t) = 0, \qquad n \neq 0,1$$

$$W_{a0}(t) = -U_T(t)\alpha(t) - \Delta\dot{h} + U_P(t) - \bar{a}(bR)\,\Delta\dot{\alpha}(t)$$

$$W_{a1}(t) = (bR)\,\Delta\dot{\alpha}(t)$$

$$\bar{\phi} = \cos^{-1}(x^*/bR), \qquad (0 \leq \bar{\phi} \leq \pi, -bR \leq x^* \leq bR) \tag{2}$$

In addition to the upwash velocity $W_a(\bar{\phi},t)$ on the reference airfoil, there is also a downwash velocity component $\lambda(x^*,t)$ due to the shed wake, $\Upsilon_{WN}(\xi^*,t)$, where $n = 0, NL$, and a downwash velocity component $W_b(x^*,t)$ due to bound vortices representing the surface of the airfoil, $\Upsilon_b(\xi^*,t)$.

Application of the Biot-Savart law yields

$$W_b(x^*,\tau) = (-1/2\pi)\int_{-bR}^{bR}[\Upsilon_b(\xi^*,\tau)/(\xi^* - x^*)]\,d\xi^*$$

$$\lambda(x^*,\tau) = (-1/2\pi)\sum_{n=0}^{NL}\int_{bR-2n\pi r}^{X_n^*(\tau)}\{\Upsilon_{WN}(\xi^*,\tau)(\xi^* - x^*)/$$

$$[(\xi^* - x^*)^2 + (nH^*)^2]\}\,d\xi^* \tag{3}$$

where H^* represents the dimensional wake spacing between successive wake layers. The wake airfoils are purely imaginary and are introduced only to model the effects due to their wake. These imaginary wake airfoils are only visual aids employed to help one write a relationship between the vortex strength in the wake layers beneath the reference airfoil and the wake vortices directly behind it. These airfoils do not represent physical surfaces over which discontinuities in velocity are produced, nor is there a bound vortex system associated with these airfoils.

The flow tangency condition can be written as

$$(1/2\pi)\int_{-1}^{1}[\Upsilon_b(\xi,\tau)/(\xi - x)]\,d\xi = -[W_a(\tau) + \lambda(\tau)] \tag{4}$$

where $\xi = (\xi^*/bR)$ and $x = (x^*/bR)$ are nondimensional chordwise variables. The Kutta condition for unsteady flow requires that the bound vortex at the trailing edge be finite. Application of the Söhngen inversion integral yields

$$\Upsilon_b(x^*,\tau) = (-2/\pi)\sqrt{(bR - x^*)/(bR + x^*)} \times \int_{-bR}^{bR}\sqrt{(bR + \xi^*)/(bR - \xi^*)}\,[-(W_a + \lambda)/(x^* - \xi^*)]\,d\xi^* \tag{5}$$

This leads to the solution for Υ_b in terms of a Glauert series

$$\Upsilon_b(\bar{\phi},\tau) = -2\sum_{m=0}^{\infty}[\lambda_m(\tau) + W_{am}(\tau)]f_m(\bar{\phi}) \tag{6}$$

where

$$f_m(\bar{\phi}) = \begin{cases} \tan(\bar{\phi}/2) & m = 0 \\ \sin(m\bar{\phi}) & m \geq 1 \end{cases} \tag{7}$$

Hence the expression for the bound circulation can be written as

$$\Gamma = \int_{-bR}^{bR}\Upsilon_b(z^*,\tau)\,dz^* = -2\pi(bR)[(W_{a0} + 1/2W_{a1}) + (\lambda_0 + 1/2\lambda_1)] \tag{8}$$

The bound vortex Υ_b can be separated into two parts corresponding to circulatory, Υ_{bc}, and noncirculatory, Υ_{bnc}, vortex distributions. The circulatory vortex Υ_{bc} accounts for the total circulation around the airfoil; however, it corresponds to zero downwash velocity $W_b = 0.0$ everywhere on the airfoil. Therefore, the circulatory bound vortex system will have no effect on the flow tangency boundary condition over the airfoil except at the trailing edge. The noncirculatory vortex system Υ_{bnc} accounts for the total downwash velocity over the airfoil; however, it produces zero circulation Γ around the airfoil. Thus, the following expressions are obtained:

$$\int_{-bR}^{bR}\Upsilon_{bc}(\xi^*,\tau)\,d\xi^* = \Gamma$$

$$\int_{-bR}^{bR}\Upsilon_{bnc}(\xi^*,\tau)\,d\xi^* = 0$$

$$(1/2\pi)\int_{-bR}^{bR}[\Upsilon_{bc}(\xi^*,\tau)/(x^* - \xi^*)]\,d\xi^* = 0$$

$$(1/2\pi)\int_{-bR}^{bR}[\Upsilon_{bnc}(\xi^*,\tau)/(x^* - \xi^*)]\,d\xi^* = W_b(x^*,\tau) = -(W_a + \lambda) \tag{9}$$

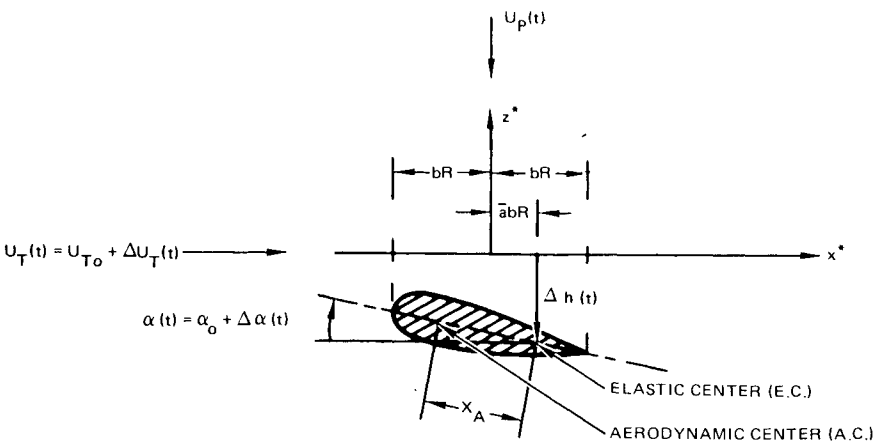

Fig. 2 Geometry of motion for a typical airfoil.

which also imply

$$\Upsilon_{bc}(\bar{\phi},\tau) = [-2/\sin(\bar{\phi})][(W_{a0} + 1/2W_{a1}) + (\lambda_0 + 1/2\lambda_1)]$$
$$\Upsilon_{bnc}(\bar{\phi},\tau) = [2/\sin(\bar{\phi})][(W_{a0} + \lambda_0)\cos(\bar{\phi}) + 1/2(W_{a1} + \lambda_1)\cos(2\bar{\phi})] - 2\sum_{m=2}^{\infty}(W_{am} + \lambda_m)\sin(m\bar{\phi}) \quad (10)$$

The unsteady Bernoulli's equation is used to obtain pressure difference $(P_u - P_\ell)$ over the airfoil and the expressions for lift and moment

$$(P_u - P_\ell) = -\rho_A\left[U_T(\tau)\Upsilon_b(x^*,\tau) + \frac{\partial}{\partial\tau}\int_{-bR}^{x^*}\Upsilon_b(\xi^*,\tau)\,d\xi^*\right]$$
$$L(\tau) = \int_{-bR}^{bR} -(P_u - P_\ell)\,dx^* = \rho_A\left\{U_T(\tau)\Gamma(\tau) - \frac{d}{d\tau}[\Gamma_{NC}^{(1)}(\tau) - \Gamma_C^{(1)}(\tau)]\right\}$$
$$M(\tau) = \int_{-bR}^{bR}(P_u - P_\ell)(x^* - \bar{a}bR)\,dx^* = -\rho_A\left\{U_T(\tau)\Gamma^{(1)}(\tau) - 1/2\frac{d}{d\tau}[\Gamma_{NC}^{(2)}(\tau) + \Gamma_C^{(2)}(\tau)]\right\} \quad (11)$$

where the lift and moment are defined as positive in the upward and pitch-up directions, respectively.

Subsequently, the lift and moment are expressed in terms of integrals associated with bound vortex Γ, $\Gamma^{(1)}$, $\Gamma_{NC}^{(1)}$, $\Gamma_{NC}^{(2)}$, $\Gamma_C^{(2)}$ to yield the relations given below:

$$\Gamma(\tau) = \int_{-bR}^{bR}\Upsilon_{bc}(\xi^*,\tau)\,d\xi^* = -(2\pi)(bR)[(W_{a0} + 1/2W_{a1}) + (\lambda_0 + 1/2\lambda_1)]$$
$$\Gamma^{(1)}(\tau) = \int_{-bR}^{bR}(\xi^* - \bar{a}bR)\Upsilon_b(\xi^*,\tau)\,d\xi^* = -(2\pi)(bR)^2 \times\{-(1/2 + \bar{a})[(W_{a0} + 1/2W_{a1}) + (\lambda_0 + 1/2\lambda_1)] + (1/4)[(W_{a1} + W_{a2}) + (\lambda_1 + \lambda_2)]\}$$
$$\Gamma_{NC}^{(1)}(\tau) = \int_{-bR}^{bR}\xi^*\Upsilon_{bnc}(\xi^*,\tau)\,d\xi^* = (2\pi)(bR)^2[(1/2)(W_{a0} - 1/2W_{a2}) + (1/2)(\lambda_0 - 1/2\lambda_2)]$$
$$\Gamma_C^{(1)}(\tau) = \int_{-bR}^{bR}(bR - \xi^*)\Upsilon_{bc}(\xi^*,\tau)\,d\xi^* = (bR)\Gamma(\tau) \quad (12a)$$

$$\Gamma_{NC}^{(2)}(\tau) = \int_{-bR}^{bR}(\xi^{*2} - 2\bar{a}bR)\Upsilon_{bnc}(\xi^*,\tau)\,d\xi^* = -(2\pi)(bR)^3 \times\{\bar{a}[(W_{a0} - 1/2W_{a2}) + (\lambda_0 - 1/2\lambda_2)] - (1/8)[W_{a1} - W_{a3}) + (\lambda_1 - \lambda_3)]\}$$
$$\Gamma_C^{(2)}(\tau) = \int_{-bR}^{bR}(\xi^{*2} - 2\bar{a}bR)\Upsilon_{bc}(\xi^*,\tau)\,d\xi^* = (1/2)(bR)^2\Gamma(\tau) \quad (12b)$$

Aerodynamic Loads in the Laplace Domain

The expressions of the unsteady air loads derived in the previous section are in terms of the Fourier coefficients of the induced downwash velocity and their time derivatives. Furthermore, the wake-induced downwash velocity is a function of the strength of the unsteady shed wake vortices in the wake layers behind and beneath the blade. A solution for the strength of these shed vortices determines the unsteady aerodynamic loads.

The coefficients of the Fourier series representing the downwash velocity λ are calculated using

$$\lambda_m(\tau) = (2/\pi)\int_0^{\pi}\lambda(\bar{\theta},\tau)\cos(m\bar{\theta})\,d\bar{\theta}$$
$$\lambda_0(\tau) = (1/2)\lambda_m(\tau)|_{m=0} \quad (13)$$

The coefficients λ_m are given by

$$\lambda_m(\tau) = (-1/bR\pi)\sum_{n=0}^{NL}\int_{bR-2n\pi r}^{X_n^*(\tau)} I(\xi^*{:}n,m)\Upsilon_{WN}(\xi^*,\tau)\,d\xi^* \quad (14)$$

where the expression for the kernel function $I(\xi^*{:}n,m)$ is

$$I(\xi^*{:}n,m) = (bR/\pi)\int_0^{\pi}\{[(\xi^* - bR\cos\bar{\theta})\cos m\bar{\theta}]/[(\xi^* - bR\cos\bar{\theta})^2 + (nH^*)^2]\}\,d\bar{\theta} \quad (15)$$

where $I(\xi^*{:}n,m)$ represents the influence of a unit vortex lying on the nth vortex sheet at ξ^*, and on the mth Fourier coefficient of the wake-induced velocity over the airfoil chord.

The wake vortex $\Upsilon_{WN}(\xi^*,\tau)$ can be related to the vortex shed at the trailing edge Υ_t at some previous time t'. The shed vortex Υ_t is only a function of time. At time $t = \tau$, the vortex shed from the trailing edge of the airfoil, in the nth wake layer, at a prior time $t = 0$ is located at $X_n^*(\tau)$, which is given by

$$X_n^*(\tau) = bR - 2n\pi r + \int_0^{\tau}U_T(t')\,dt' \quad (16)$$

At a time $t = \tau$, the location of a vortex shed from the trailing edge of the airfoil at some previous time $t = t'$ is given by $\xi^*(\tau,t',n)$

$$\xi^*(\tau,t',n) = bR - 2n\pi r + \int_{t'}^{\tau}U_T(t)\,dt \quad (17)$$

In linear unsteady aerodynamic theories it is common practice to impose the tangent flow boundary condition on the X^* axis instead of the moving airfoil surface. In an analogous manner, the time-varying velocity term appearing in the positions of the wake vortices will be approximated by the mean value:

$$X_n^*(\tau) = bR - 2n\pi r + (\tau)U_{TO}$$
$$\xi_n^*(\tau,t',n) = bR - 2n\pi r + (\tau - t')U_{TO} \quad (18)$$

The condition of zero pressure discontinuity across the wake requires the vortices shed at the trailing edge to travel downstream with the time-varying freestream velocity. This condition is imposed in its exact form; thus,

$$d\xi/dt' = -U_T(t') \text{ or } d\xi^* = -U_T(t')\,dt' \quad (19)$$

Using Eqs. (18) and (19) together with Eqs. (14) and (15) yields[5]

$$\lambda_m(\tau) = (-1/bR\pi)\sum_{n=0}^{NL}\int_0^{\tau} I[(\tau - t'){:}n,m](\Upsilon_t(t')U_T(t'))\,dt' \quad (20)$$

$$\dot{\lambda}_m(\tau) = (-1/bR\pi)\sum_{n=0}^{NL}\int_0^{\tau}\frac{\partial}{\partial(\tau)}\{I[(\tau - t'){:}n,m]\} \times[\Upsilon_t(t')U_T(t')]\,dt' - (1/bR\pi)I[t = 0{:}0,m][\Upsilon_t(\tau)U_T(\tau)] \quad (21)$$

where

$$I[(\tau - t'):n,m] = [T_{sc}/\pi] \times \int_0^{\tau} \left[\{[(\tau - t') + (T_{sc}) - n(T_R) - (T_{sc})\cos\bar{\theta}]\cos(m\bar{\theta})\}/ \{[(\tau - t') + (T_{sc}) - n(T_R) - (T_{sc})\cos\bar{\theta}]^2 + (nT_H)^2\} \right] d\bar{\theta} \quad (22)$$

The introduction of the parameters T_{sc},T_R, and T_H is primarily a matter of convenience; where T_{sc} is the time required for a fluid particle to travel one semichord length with the velocity U_{TO}, $T_{sc} = [(bR)/U_{TO}]$,T_R is the period of revolution of the rotor, $T_R = (2\pi/\Omega) = (2\pi r/U_{TO})$, and T_H is the time required for a fluid particle to travel one wake spacing with the speed U_{TO}, $T_H = H^*/U_{TO}$.

Introducing a new kernel function for $\dot{\lambda}_m$ and performing the integrations associated with this function leads to

$$\dot{\lambda}_m(\tau) = [-U_T(\tau)/\pi(bR)^2] \sum_{n=0}^{NL} \int_0^{\tau} D[(\tau - t'):n,m] \times [\Upsilon_t(t')U_T(t')]\, dt' - (m/\pi bR)\frac{d}{d\tau}[\Gamma(\tau)] \quad (23)$$

where

$$D[(\tau - t'):n,m] = [(T_{sc})^2/\pi] \int_0^{\pi} [\{(nT_H)^2 - [(\tau - t') + T_{sc} - nT_R - T_{sc}\cos\bar{\theta}]^2\}/ \{[(\tau - t') + T_{sc} - nT_R - T_{sc}\cos\bar{\theta}]^2 + (nT_H)^2\}^2] \cos(m\bar{\theta})\, d\bar{\theta}$$

$$\times D[(\tau - t'):n,m] = T_{sc}\frac{d}{d\tau} I[(\tau - t'):n,m] \quad (24)$$

Expressing the lift in terms of its quasisteady, noncirculatory, and wake contributions yields

$$L(\tau) = L_Q(\tau) + L_{NC}(\tau) + L_W(\tau) = L_C(\tau) + L_{NC}(\tau) \quad (25)$$

where

$$[L_C(\tau)/2\rho_A U_T(\tau)] = (1/2) \int_0^{\tau} \left[\sum_{n=0}^{NL} \{(1/2)D[(\tau - t'):n,0] - (1/2)D[(\tau - t'):n,2]\} - 1 \right] [\Upsilon_t(t')U_T(\tau')]\, dt' \quad (26)$$

$$L_{NC}(\tau) = -(\pi)\rho_A(bR)^2\dot{W}_{a0} \quad (27)$$

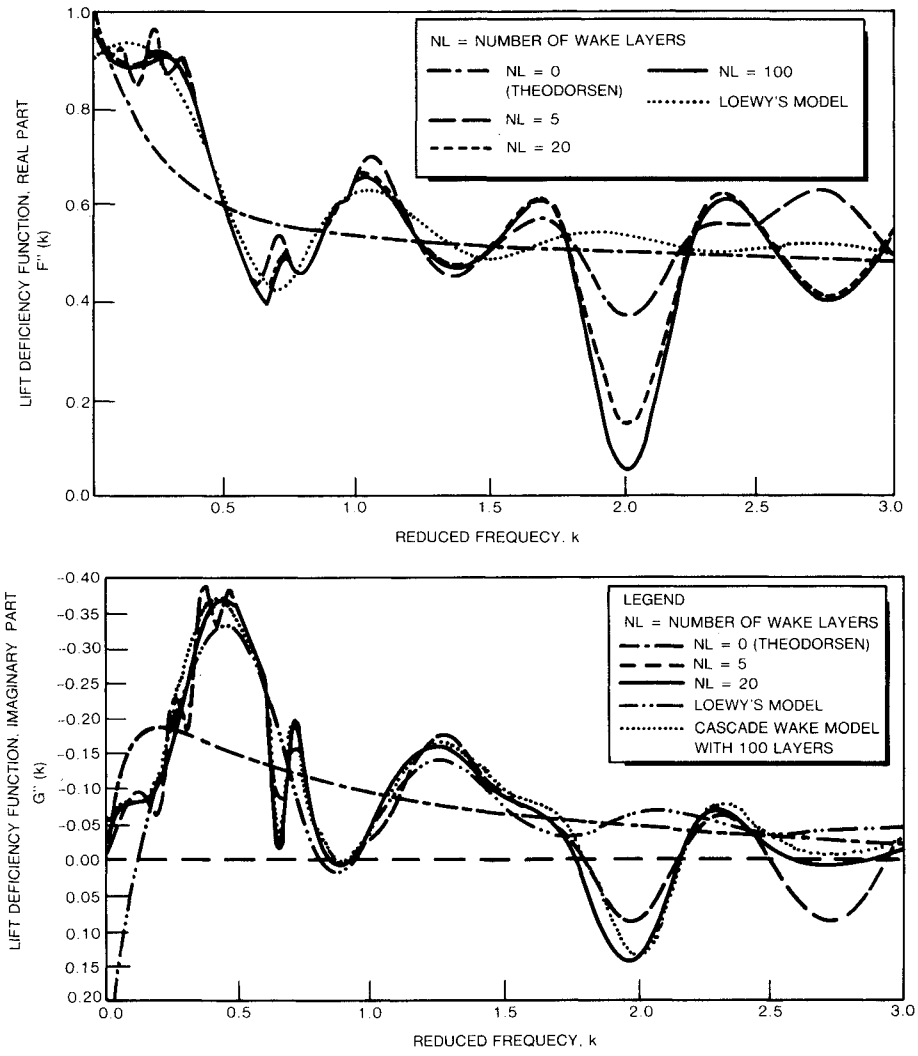

Fig. 3 Cascade-wake lift deficiency function for increasing numbers of wake layers ($\bar{T}_{Re} = 9.4248$, $\bar{T}_{He} = 1.5707$; $\bar{r}_e = 1.5$, $\bar{h}_e = 1.5707$) and its comparison with Loewy's theory.

Applying Kelvin's law of conservation of the circulation yields the following expression for the quasisteady lift:

$$[L_Q(\tau)/2\rho_A U_T(\tau)] = \pi(bR)Q(\tau) = -\int_0^\tau \left[\sum_{n=0}^{NL} \{(1/2)I[(\tau - t'):n,0] + (1/2)I[(\tau - t'):n,1\} + (1/2)\right][\Upsilon_t(t')U_T(t')]\, dt' \quad (28)$$

where $Q(\tau)$ is the 3/4-chord-point downwash velocity given by

$$Q(\tau) = -(W_{a0} + 1/2W_{a1}) = \{U_T(\tau)[\alpha_0 + \Delta\alpha(t)] + \Delta\dot{h} - U_p(t) + bR(1/2 - \bar{a})\,\Delta\dot{\alpha}(t)\} \quad (29)$$

It is important to note that both Eqs. (26) and (28) are in convolution form, and they involve the unknown trailing edge vortex strength multiplied by the time-varying velocity $[\Upsilon_t(t')U_T(t')]$. Therefore, the Laplace transform can be used to eliminate the unknown $[\Upsilon_t(t')U_T(t')]$, and one obtains the following relation in the Laplace domain

$$\mathcal{L}[L_C(\tau)/2\pi\rho_A(bR)U_T(\tau)] = C''\mathcal{L}\{Q(\tau)\} \quad (30)$$

where the generalized cascade lift deficiency function C'', which acts as a Laplace domain operator relating the 3/4-chord downwash velocity to the circulatory portion of the lift, is given by

$$C'' = -\left(\frac{1}{2}\right)\left[\frac{\mathcal{L}\left\{\sum_{n=0}^{NL}[\frac{1}{2}D(t:n,0) - \frac{1}{2}D(t:n,2)] - 1\right\}}{\mathcal{L}\left\{\sum_{n=0}^{NL}[\frac{1}{2}I(t:n,0) + \frac{1}{2}I(t:n,1)] + \frac{1}{2}\right\}}\right] \quad (31)$$

It was shown in Ref. 5 that a further simplification of the expression for $C''(s)$ [Eq. (31)] is possible. Therefore, after additional algebraic manipulation $C''(s)$ one obtains

$$C''(\bar{s},\bar{T}_R,\bar{T}_H) = \frac{\left[K_1(\bar{s}) - (\bar{s}/2)\sum_{n=1}^{NL} e^{-n\bar{T}_R\bar{s}}[F(\bar{s}:n,0,\bar{T}_R,\bar{T}_H) - F(\bar{s}:n,2,\bar{T}_R,\bar{T}_H)]\right]}{\left[[K_1(\bar{s}) + K_0(\bar{s})] + \sum_{n=1}^{NL} e^{-n\bar{T}_R\bar{s}}[F(\bar{s}:n,0,\bar{T}_R,\bar{T}_H) + F(\bar{s}:n,1,\bar{T}_R,\bar{T}_H)]\right]} \quad (32)$$

where the expression for $\bar{F}(s:n,m,\bar{T}_R,\bar{T}_H)$ is given by

$$F(\bar{s}:n,m,\bar{T}_R,\bar{T}_H) = \int_{[1-n\bar{T}_R]}^{\infty}\left[(1/\pi)\int_0^\pi [[t' - \cos\bar{\theta}]\cos(m\bar{\theta})/\{[t' - \cos\bar{\theta}]^2 + (n\bar{T}_H)^2\}]\, d\bar{\theta}\right]e^{-\bar{s}t'}\, dt' \quad (33)$$

This Laplace-domain lift deficiency function contains two infinite summations and integrals that do not lend themselves to closed form solutions in terms of familiar mathematical functions. However, several important properties of C'' can be obtained analytically.

Reference 5 contains a mathematical proof that the limit of the lift deficiency function for the cascade-wake theory approaches Theodorsen's lift deficiency function when the wake spacing approaches infinity. It is also shown that the cascade theory becomes identical to the generalized Greenberg's theory[5] when returning wake layers are neglected ($NL = 0$).

The case of the multibladed rotor differs from the single bladed case in terms of the horizontal shift between successive wake layers, which is reduced when compared to the single bladed case. The magnitude of this wake layer shift is equal to the distance along a circular arc, measured between two airfoils (at the same radial station) on successive blades. Furthermore, the vertical wake spacing is also reduced by a factor equal to the total number of blades present in the rotors; thus, $\bar{T}_{Re} = \bar{T}_R/Q$ and $\bar{T}_{He} = \bar{T}_H/Q$.

Frequency Domain Lift Deficiency Function

The frequency domain lift deficiency function for the cascade-wake theory is required for two reasons. First, the lift deficiency function of the cascade-wake theory should be compared with Loewy's lift deficiency function in the frequency domain, so as to identify differences between these two theories. Second, finite-state time-domain models are obtained from Pade approximants of the lift deficiency function in the frequency domain. Therefore, in this section an efficient method for calculating the lift deficiency function for the cascade-wake theory in the frequency domain is presented.

Derivation

The frequency domain lift deficiency function can be obtained by replacing the nondimensional Laplace variable $\bar{s}$ by (ik). For convenience, the various integrals in the numerator and denominator of C'' are treated separately. The combined integral for the numerator will be denoted as $IN(ik:n,\bar{T}_{Re},\bar{T}_{He})$ and the combined integral for the denominator will be denoted as $ID\ (ik:n,\ \bar{T}_{Re},\ \bar{T}_{He})$

$$IN(ik:n,\bar{T}_{Re},\bar{T}_{He}) = \int_{[1-n\bar{T}_{Re}]}^{\infty}\left[(1/\pi)\int_0^\pi [[t' - \cos\bar{\theta}][1 - \cos(2\bar{\theta})]/\{[t' - \cos\bar{\theta}]^2 + (n\bar{T}_{He})^2\}]\, d\bar{\theta}\right]e^{-ikt'}\, dt' \quad (34)$$

$$ID(ik:n,\bar{T}_{Re},\bar{T}_{He}) = \int_{[1-n\bar{T}_{Re}]}^{\infty}\left[(1/\pi)\int_0^\pi [[t' - \cos\bar{\theta}][1 + \cos(\bar{\theta})]/\{[t' - \cos\bar{\theta}]^2 + (n\bar{T}_{He})^2\}]\, d\bar{\theta}\right]e^{-ikt'}\, dt' \quad (35)$$

The upper limits of the outer integrals in IN and ID are infinity. This implies that in the present model the wake would extend to infinity behind the imaginary airfoils when dealing with the case of simple harmonic motion. However, only the wake contained within some double azimuth angle straddling the blade on both sides can be approximated to lie on the same plane as the blade section. This limits the length of the wake to be considered for idealized two-dimensional theory. We shall assume that only the vortices contained within an azimuth angle $(2\pi/Q)$, which is the angle between two successive blades, straddling the reference blade, are important for the wake layers beneath the rotor. Several numerical experiments with

different wake lengths were carried out to verify the validity of this assumption. Therefore, the limits of integration for the outer integrals in *IN* and *ID* are adjusted so as to account for this assumption. Subsequently, the region of the wake layers beneath the reference airfoil to be included in the computations lie on $-(2\pi r/Q) \le \xi_n^* \le (2\pi r/Q)$. However, the integration in *IN* and *ID* are in terms of time. An equivalent expression to Eqs. (18) for a change of variable from the position of vortices ξ_n^* in the nth wake layer of a Q-bladed rotor to a time variable t' can be obtained[5]:

$$\xi_n^* = bR - (2\pi rn/Q) + \Omega rt \tag{36}$$

$$t = T_{sc}[t' - (1 - n\bar{T}_{Re})] \tag{37}$$

Using these relations, one obtains

$$\xi^* = 2\pi r/Q \text{ corresponds to } t' = \bar{T}_{Re} \tag{38}$$

$$\xi^* = -2\pi r/Q \text{ corresponds to } t' = -\bar{T}_{Re}$$

Therefore, the limits of integration for outer integrals in *IN* and *ID* are modified so that the upper limit of the outer integral is $\bar{T}_{Re}$ and the lower limit of the outer integral is given by the quantity $-a$, where

$$a = \begin{cases} \bar{T}_{Re} & \text{for } n \neq 1 \\ \bar{T}_{Re} - 1 & \text{for } n = 1 \end{cases} \tag{39}$$

The integrands in *IN* and *ID* are well behaved and have no singularity in the region of the integration. Therefore, the integration in the rectangular region of $0 \le \theta \le \pi, -a \le t' \le \bar{T}_{Re}$ can be treated using any available numerical integration technique, such as Gaussian quadrature or adaptive Romberg extrapolation algorithms.

Computational Aspects

In actual applications, these integrals have to be evaluated numerically for a large number of wake layers and at different values of the reduced frequency k so as to generate plots of $C''(k)$. Such calculations require a considerable amount of computer time; therefore, expressions approximating the integrands of *IN* and *ID* for wake layers sufficiently far removed from the rotor disk were developed. In Ref. 5 it has been shown that the integrand of the outer integral in *IN* is an odd function of t', and therefore, *IN* for $n = 1$ reduces to

$$IN(ik{:}n,\bar{T}_{Re},\bar{T}_{He}) = -(2i)\int_0^{\bar{T}_{Re}} \times \left[(1/\pi)\int_0^{\pi} [[t' - \cos\bar{\theta}][1 - \cos(2\bar{\theta})]/ \{[t' - \cos\bar{\theta}]^2 + (n\bar{T}_{He})^2\}]\, d\bar{\theta}\right] \sin(kt')\, dt' \text{ for } n \neq 1 \tag{40}$$

This equation reveals two separate important properties of *IN*:

1) *IN* approaches zero as k approaches either zero or infinity, irrespective of the wake layer index n, i.e.,

$$\lim_{k \to 0} IN(ik{:}n,\bar{T}_{Re},\bar{T}_{He}) = 0 \tag{41}$$

$$\lim_{k \to \infty} IN(ik{:}n,\bar{T}_{Re},\bar{T}_{He}) = 0 \tag{42}$$

This property is important for determining the limiting values of C'' as k approaches zero or infinity.

2) The real part of *IN* is always zero, and *IN* is purely an imaginary number.

For wake layers sufficiently far from the rotor disk, an accurate closed form approximate solution can be obtained by using binomial expansion, which eliminates the need for numerical integration.[5] This approximation is for wake layers below nth wake layer, where n is constrained by

$$n \ge [100]^{1/4}\{[\bar{T}_{Re}]/[n\bar{T}_{He}]\} \tag{43}$$

Comparison with Loewy's Theory

The numerical results presented in this section provide a comparison with Loewy's theory. The nondimensional horizontal wake shift and nondimensional vertical wake spacing parameters selected for the numerical examples presented in this paper are $\bar{T}_{Re} = 9.4248$ and $\bar{T}_{He} = 1.5707$. This case corresponds to a blade section of radial distance 0.3R of a four-bladed rotor with a semichord $bR = 0.05$R operating at an inflow ratio of 0.05 or thrust coefficient of 0.005. The corresponding parameters for Loewy's theory are $\bar{r}_e = 1.500$ and $\bar{h}_e = 1.5707$. For this case, the integer frequency ratio will occur at the reduced frequencies $k = 0.666$, 1.333, 2.000, 2.666,...(0.666m), where m is any integer.

The real and imaginary parts of the cascade-wake lift deficiency function, for various values of reduced frequency, were calculated using a combined analytical and numerical method described in the previous section. The contributions of the first 20 wake layers were calculated using numerical integration, and approximate closed-form solutions were used for the remaining wake layers. The real and imaginary parts of the cascade-wake theory lift deficiency function are plotted against the reduced frequency in Fig. 3 for an increasing number of wake layers. The number of wake layers beneath the rotor disk *NL* has been varied from 0 to 100. The case without any returning wake layers beneath the rotor, $NL = 0$, is identical to Theodorsen's theory. Figure 3 shows that there is a large difference due to the returning wakes (i.e., $NL > 0$), and the primary effect is due to the first 20 wake layers. Furthermore, the imaginary part of the lift deficiency function seems to converge faster than the real part with increasing number of wake layers. The cascade lift deficiency function exhibits peaks and valleys in the vicinity of the reduced frequencies corresponding to the integer equivalent frequency ratios, for this case $k = 0.666$, 1.333, 2.000, 2.666,...(0.666 m), where m is any integer.

The real and imaginary parts of the cascade lift deficiency function with 100 wake layers beneath the rotor are compared with Loewy's theory in Fig. 3. The cascade lift deficiency function agrees very well with Loewy's lift deficiency function with two exceptions: 1) in the vicinity of the regions where $\bar{m} = (k)\cdot(\bar{r}_e)$ is an integer, and 2) near the origin where the cascade-wake theory always tends to the correct quasisteady value of unity. From these plots it is also evident that Loewy's lift deficiency function tends to reduce somewhat the effect of the returning wakes near the integer frequency ratios when compared with the cascade-wake theory. One could speculate as to the possible cause for this difference. The extension of the wake to infinity on both sides of the rotor, as done in Loewy's theory, could lead to wake cancellations at integer frequency ratios and, hence, result in reduced unsteady effects.

It should also be noted that the zero-frequency limit of Loewy's lift deficiency function for this numerical example is $C' = (0.8667 + i\ 0.2667)$, corresponding to a 9.32% reduction and 17.10 deg phase lead in circulatory loads. However, the generalized cascade lift deficiency function always approaches unity as reduced frequency goes to zero. The zero frequency limit for Loewy's lift deficiency function was calculated using the expressions derived in Ref. 5, which can also be found in Ref. 1. Previous studies dealing with zero-frequency limit of Loewy's lift deficiency function treated k and $\bar{m}_e$ as independent parameters. When $\bar{m}_e$ is treated as independent of k, as k

goes to zero, the wake weighting function involved in Loewy's lift deficiency function W remains a finite number for noninteger values of $\bar{m}_e$ and approaches infinity for integer values of $\bar{m}_e$. However, for a blade section at a given radial station, $\bar{r}_e$, $\bar{m}_e$ is not an independent function of k, ($\bar{m}_e = k \cdot r_e$). Reference 5 takes into account this dependency and develops the proper zero-frequency limit for Loewy's lift deficiency function. This limit is always different from unity and its value is dependent on $\bar{h}_e$ and $\bar{r}_e$, unlike the findings of Refs. 4 and 11. Reference 5 noted that Loewy's theory contains a jump discontinuity at $k = 0$ in the wake weighting function W. This discontinuity is associated with the validity of a certain improper integral at $k = 0$, which was used in Ref. 4. The implication of this discontinuity is that low frequency limit of C' is different from C' when evaluated exactly at $k = 0$. Although the latter is equal to unity, as expected for the steady condition, the former is a function of $\bar{h}_e$ and $\bar{r}_e$ and can lead to significant reductions in loads.

Finite State Modeling of Cascade Lift Deficiency Function

The Bode plot of the cascade lift deficiency function is shown in Fig. 4. Ten peaks and valleys are identified in Fig. 4, the odd numbers corresponding to the valleys and the even numbers corresponding to the peaks. As indicated in Refs. 8 and 9, each valley in the Bode plot indicates the presence of a pair of complex conjugate or repeated zeros, and each peak indicates the presence of a pair of complex conjugate zeros or repeated real poles. Furthermore, whenever the slopes of the asymptotes of the transfer function are equal at low and high frequencies (i.e., zero and infinity), then the transfer function has equal numbers of zeros and poles. Figure 4 shows five complex poles and five complex zeros for the cascade lift deficiency function in the frequency range of $0 \le k \le 3.0$. Furthermore, the cascade lift deficiency function has a known branch-cut on the negative real axis. A branch-cut on the negative real axis can be modeled by a finite number of real poles distributed on that axis. Hence, an approximate transfer function is constructed so as to capture the first five complex poles and zeros and the effect of the branch-cut:

$$C''(ik,\bar{T}_{Re},\bar{T}_{He}) = \frac{N(ik)}{D(ik)} = \frac{RN(k) + iIN(k)}{RD(k) + iID(k)}$$
$$= 0.5\left[\frac{(ik)^{15} + \sum_{m=1}^{15} a_m (ik)^{(15-m)}}{(ik)^{15} + \sum_{m=1}^{15} b_m (ik)^{(15-m)}}\right] \qquad (44)$$

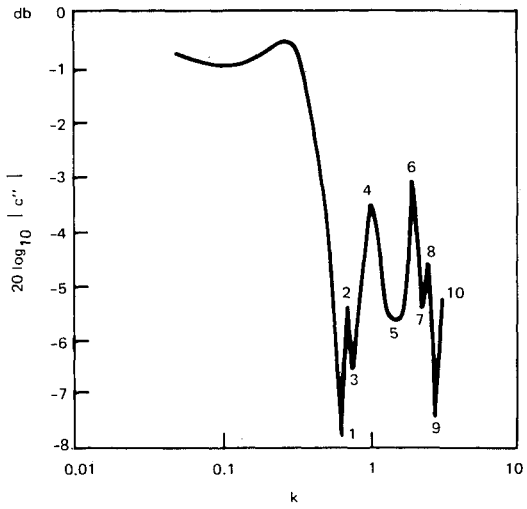

Fig. 4 Bode plot of cascade lift deficiency function for $\bar{T}_{He} = 1.5707$, $\bar{T}_{Re} = 9.4248$.

To ensure that the limit of C'' approaches unity as k tends to zero, $b_{15} = 0.5\, a_{15}$. It should also be noted that four additional real poles and zeros have been added in order to model the branch cut. The coefficients $a_1 \ldots a_{15}$, $b_1 \ldots b_{14}$ are evaluated by minimizing the error function

$$E = \sum_{j=1}^{NFR} \left\| C''(ik_j,\bar{T}_{Re},\bar{T}_{He}) - \frac{N(ik_j)}{D(ik_j)} \right\|^2 \qquad (45)$$

This leads to a nonlinear least squares problem that converges rather slowly. The Fletcher-Powell nonlinear unconstrained minimization algorithm[12] was used for the evaluation of the coefficients. In Figs. 5a and 5b, the real and imaginary parts of the approximate cascade lift deficiency function are compared with the corresponding exact values. The resulting agreement is acceptable up to $k = 1.5$. However, the procedure failed to model the very large peak and valley in the vicinity of $k = 2.0$ and a peak in the imaginary part at $k = 0.67$ (i.e., $\bar{m}_e = 1$ and 3). The main reason for this is the existence of a strong local minimum. In order to improve the accuracy, a general purpose optimization program was used. This allowed for considerable flexibility and experimentation in selecting the optimization scheme appropriate for this particular class of problems.[13] The selection of the successive unconstrained minimization strategy (SUMT) with quadratic extended interior penalty function method[14,15] and Broyden-Fletcher-Goldfarb-Shanno (BFGS) optimizer and Golden section one-dimensional search proved to be successful in dealing with the presence of many local minima. The results for (15 × 15) and (10 × 10) Pade approximants are presented in Fig. 6. While the (15 × 15) Pade approximant is more accurate, the (10 × 10) Pade approximant is more convenient for use in aeroelastic applications due to its

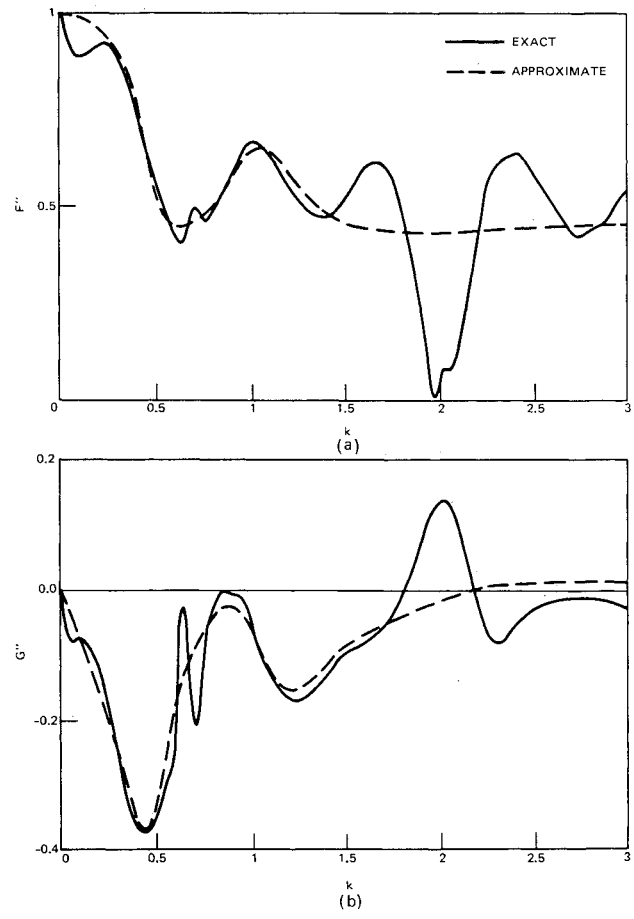

Fig. 5 Cascade lift deficiency function and its 15th order complex Pade approximant using Fletcher-Powell unconstrained minimization ($\bar{T}_{He} = 1.5707$, $\bar{T}_{Re} = 9.4248$).

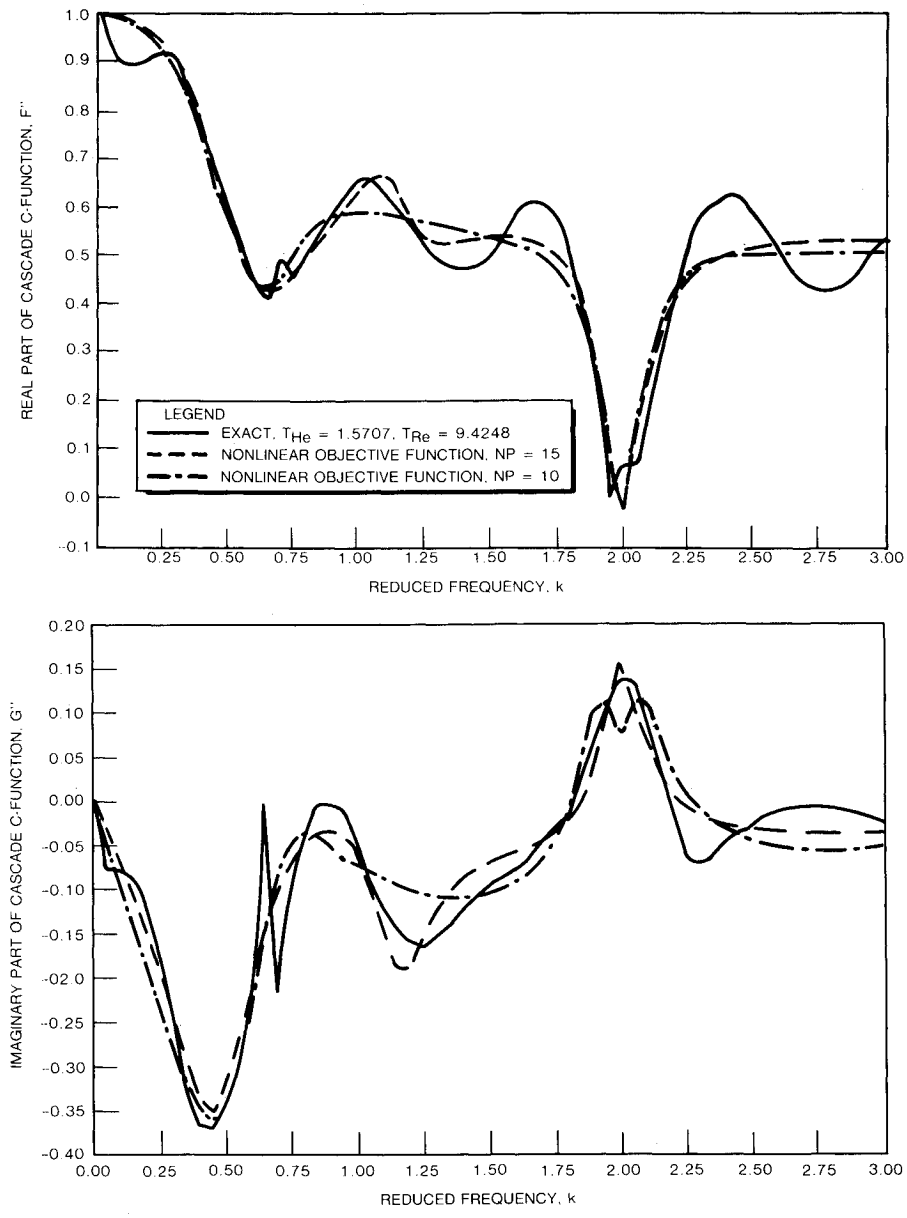

Fig. 6 Cascade lift deficiency function and its complex Pade approximant using ADS optimizer ($\bar{T}_{He}$ = 1.5707, $\bar{T}_{Re}$ = 9.4248).

Table 1 Coefficients of the approximate lift deficiency function

$N(ik)$		$D(ik)$	
a_1	0.701	b_1	0.258
a_2	7.361	b_2	7.429
a_3	4.921	b_3	1.316
a_4	11.744	b_4	12.012
a_5	5.983	b_5	−0.101
a_6	−3.852	b_6	−6.042
a_7	−9.434	b_7	−5.375
a_8	14.318	b_8	6.345
a_9	1.144	b_9	4.376
a_{10}	8.375	b_{10}	4.188

smaller size. The resulting coefficients for the (10 × 10) Pade approximant are given in Table 1.

Concluding Remarks

A cascade-wake theory was developed in both the Laplace and frequency domains. A combined numerical and analytical scheme was developed to deal with various integrals and infinite summations required and used as to study the influence of the number of the returning wake layers beneath the rotor.

The lift deficiency function for the cascade-wake model in the frequency domain was compared with that corresponding to Loewy's theory. It was found that the cascade-wake theory predicts somewhat larger unsteady aerodynamic effects at integer frequency ratios than Loewy's theory. Furthermore, the low reduced frequency limit of the cascade-wake theory tends to the correct quasisteady limit of unity. The differences between the present theory and the Loewy theory for reduced frequencies, which are different from zero, can be attributed to the differences in the wake structure that form the basis for these theories.

Using a modified Pade approximant technique suitable for rotary wings, finite-state time-domain representations of the cascade theory are developed. Such time-domain models are useful for generating indicial response functions for rotary wings in hover, which are applicable to the study of unsteady flight conditions such as maneuvers and gusts. Furthermore, the time-domain aerodynamics also have potential applications to the study of active control systems intended for suppressing aeroelastic instabilities in hover.

Acknowledgments

This research was partially supported by NASA Ames Research Center under NASA Grant NAG 2-209. The constructive comments of the grant monitor Dr. W. Warmbrodt are gratefully acknowledged.

References

[1]Dinyavari, M. A. H. and Friedmann, P. P., "Unsteady Aerodynamics in Time and Frequency Domains for Finite Time Arbitrary Motion of Rotary Wings in Hover and in Forward Flight," *Proceedings of AIAA/ASME/ASCE/AHS 25th Structures, Structural Dynamics, and Materials Conference*, AIAA, New York, Vol. 2, May 1984, pp. 226–282.

[2]Greenberg, J. M., "Airfoil in Sinusoidal Motion in Pulsating Stream," NACA TN-1326, 1947.

[3]Dinyavari, M. A. H. and Friedmann, P. P., "Application of Time-Domain Unsteady Aerodynamics to Rotary-Wing Aeroelasticity," *AIAA Journal*, Vol. 24, Sept. 1986, pp. 1424–1432.

[4]Loewy, R. G., "A Two-Dimensional Approximation to the Unsteady Aerodynamics of Rotary Wings," *Journal of Aeronautical Sciences*, Vol. 24, Feb. 1957, pp. 81–92.

[5]Asghar-Hessari-Dinyavari, M., "Unsteady Aerodynamics in Time and Frequency Domains for Finite-Time Arbitrary-Motion of Helicopter Rotor Blades in Hover and Forward Flight," Ph.D. Dissertation, Univ. of California, Los Angeles, CA, March 1985.

[6]Dowell, E. H., "A Simple Method for Converting Frequency Domain Aerodynamics to the Time Domain," NASA TM-81844, 1980.

[7]Vepa, R., "Finite-State Modeling of Aeroelastic Systems," Ph.D. Dissertation, Stanford Univ., Stanford, CA, May 1975.

[8]Venkatesañ, C. and Friedmann, P. P., "A New Approach to Finite State Aerodynamics Modeling," *AIAA Journal*, Vol. 24, Dec. 1986, pp. 1889–1897.

[9]Venkatesañ, C. and Friedmann, P. P., "Finite State Modeling of Unsteady Aerodynamics and Its Application to a Rotor Dynamic Problem," School of Engineering and Applied Science, Univ. of California, Los Angeles, CA, UCLA-ENG-85-10, March 1985.

[10]Hammond, C. E., "Compressibility Effects in Helicopter Rotor Flutter," Ph.D. Thesis, Georgia Institute of Technology, Atlanta, GA, 1969.

[11]Johnson, W., *Helicopter Theory*, Princeton Univ., Princeton, NJ, 1980, pp. 526–535.

[12]Kuester, J. L. and Mize, J. H., *Optimization Techniques with Fortran*, McGraw-Hill, New York, 1973, pp. 355–366.

[13]Vanderplaats, G. N., "ADS—A Fortran Program for Automated Design Synthesis," Univ. of California, Santa Barbara, CA, Version 1.00, 1984.

[14]Broydon, C. G., "The Convergence of a Class of Double Rank Minimization Algorithms," Pts. I and II, *Journal of the Institute of Mathematics and Its Applications*, Vol. 6, 1970, pp. 76–90 and 222–231.

[15]Fletcher, R., "A New Approach to Variable Metric Algorithms," *Computer Journal*, Vol. 13, 1970, pp. 317–322.

[16]Goldfarb, D., "A Family of Variable Metric Methods Derived by Variational Means," *Maths. Comput.*, Vol. 24, 1970, pp. 23–36.

[17]Shanno, D. F., "Conditioning of Quasi-Newton Methods for Function Minimization," *Maths. Comput.*, Vol. 24, 1970, pp. 647–656.